



# Further insight into the molecular basis of carotenoid–albumin interactions: circular dichroism and electronic absorption study on different crocetin–albumin complexes

Ferenc Zsila,\* Zsolt Bikádi and Miklós Simonyi

Department of Molecular Pharmacology, Institute of Chemistry, Chemical Research Center, POB 17, 1525 Budapest, Hungary

Received 31 January 2002; accepted 21 February 2002

**Abstract**—Binding of the achiral carotenoid crocetin to the serum albumins of seven different species in borate buffer at pH 8.5 was studied in detail by UV–vis circular dichroism and absorption spectroscopy. The circular dichroism spectra yielded new information about this carotenoid–protein interaction showing the inter- and intramolecular types of induced chirality. In the visible region, human and pig albumin–crocetin complexes exhibited intense, bisignate, vibrationally coupled circular dichroism bands with opposite chirality proving intermolecular excitonic interaction between the bound crocetin molecules, left-handed for human and right-handed for pig albumin, respectively. This sign inversion and the very weak excitonic bands found with dog, horse and rat albumin were interpreted with the model of two carotenoid molecules fitted to the fatty acid binding sites of human albumin in subdomain IIIA. Positive and negative Cotton effects measured around 315–325 nm indicate that the *cis*-isomers of crocetin also bind to serum albumin and they become optically active due to the distortion around the *cis*-bond induced by the surrounding protein structure and producing inherently chiral, non-planar conformers. To determine the sense of the resulting molecular helicity the  $C_2$ -chirality rule was applied. In all cases, albumin binding caused a bathochromic shift of the visible absorption band of crocetin due to dispersion interactions although the bandwidth and the vibrational fine structure were distinctly altered depending on the kind of albumin used. For human, bovine, rabbit and rat serum albumins the better resolved vibrational structure suggests a few, high affinity binding sites with rigid environments restricting conformational mobility of their ligands while the increased bandwidth and the suppressed fine structure obtained by titration of crocetin solution with horse, pig and dog albumins point to heterogeneous binding sites with lower affinity. © 2002 Elsevier Science Ltd. All rights reserved.

## 1. Introduction

Carotenoids are plant pigments found in vegetables and fruits as common components of the human diet. Saffron, the dry stigmas of the plant *Crocus sativus* L. is currently used as a spice and food colorant and is also applied to treat various diseases in traditional and modern medicine.<sup>1,2</sup> As has been demonstrated, crocetin (Fig. 1) the main constituent of saffron extract can be used as an antitumour agent in cancer chemotherapy.<sup>3–5</sup> Experimental evidence has also shown that intravenous injection of the sodium salt of *trans*-crocetin enhances systemic O<sub>2</sub> transport and tissue oxygenation.<sup>6</sup> In the course of such treatments, crocetin transported by blood may interact with different plasma proteins which can modify its biological effects. Additionally, crocetin can be used as a molecular probe

to provide valuable information on the topology and stereochemistry of protein binding sites. As demonstrated in our preceding paper,<sup>7</sup> crocetin binds preferentially to human serum albumin and exhibits a well-defined induced circular dichroic spectrum with two major bands of opposite sign, proving intermolecular excitonic interaction between carotenoids bound to the albumin molecule. According to the exciton chirality rule, the signs of the bisignate CD curve proved that the long axes of the interacting crocetin molecules form a negative (counterclockwise) intermolecular angle (left-handed chirality).<sup>8</sup> Furthermore, crocetin binding was accompanied by a significant red shift in its visible absorption spectrum indicating the high polarizability of the protein environment. In accord with earlier observations,<sup>9</sup> CD titration experiments performed with palmitic acid indicated that crocetin and long-chain fatty acids have common binding sites on HSA. Based on the X-ray crystallographic structure of HSA complexed with palmitic acid<sup>10–12</sup> we proposed a model suggesting that binding of two crocetin molecules to the

\* Corresponding author. Fax: (+36) 1-325-7750; e-mail: [zsferi@chemres.hu](mailto:zsferi@chemres.hu)

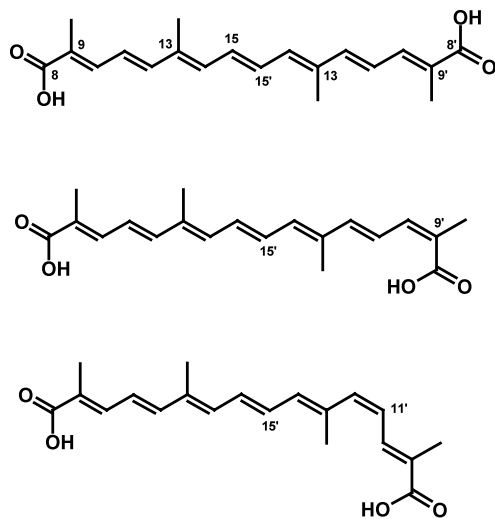


**Figure 1.** Chemical structure of all-*trans*, 9'-*cis* and 11'-*cis* crocetin (8,8'-diapocarotene-8,8'-dioic acid).

fatty acid sites 3 and 4 of subdomain IIIA might be responsible for the observed intermolecular exciton coupling.<sup>7</sup>

Despite the great importance of carotenoids in human health their interaction with plasma proteins is poorly understood and unexplored at a molecular level. This fact makes the study of serum albumin–crocetin complexes of considerable interest. Therefore, we extended our spectroscopic investigations to other serum albumins, namely dog, horse, bovine, pig, rat and rabbit albumin showing 79.3, 76.2, 75.6, 75 and 73.2% pair-

wise sequence identities with HSA<sup>13</sup> (the primary sequence of rabbit albumin has not yet been determined). In addition to HSA, only horse albumin was subjected to X-ray crystallographic measurements revealing its tertiary structure to be highly similar to human albumin.<sup>14</sup>

## 2. Results and discussion

Fig. 2 shows the electronic absorption spectrum of all-*trans* crocetin between 205 and 550 nm in aqueous buffer solution at pH 8.5. In the visible region, the vibronically structured intense absorption band corresponds to the electronically allowed  $1^1A_g \rightarrow 1^1B_u$  transition ( $S_0 \rightarrow S_2$ ) having a transition moment oriented along the long axis of the conjugated chain.<sup>15</sup> According to the second derivative spectrum, the vibronic progression is  $\sim 1470 \text{ cm}^{-1}$  reflecting the excitation of the C=C stretching mode. Since the all-*trans* crocetin molecule has perfect  $C_{2h}$  symmetry, the  $1^1A_g \rightarrow 1^1A_g$  excitation ( $S_0 \rightarrow S_3$ ), having a transition moment perpendicular to the former one, is optically forbidden and becomes electronically allowed only for *cis*-isomers (Fig. 1).<sup>16</sup> The weak band at 311.6 nm (Fig. 2) corresponds to this transition, indicating the presence of a minor fraction of various *cis*-isomers. It is well known that the  $S_0 \rightarrow S_2$  transition, having a large transition dipole moment, is strongly affected by the polarizability of the environment; increasing solvent polarizability lowers the  $S_0 \rightarrow S_2$  excitation energy through induced dipole-induced dipole (dispersion) interactions.<sup>17</sup> An analogous mechanism is responsible for the red shift in the absorption spectrum when carotenoid molecules

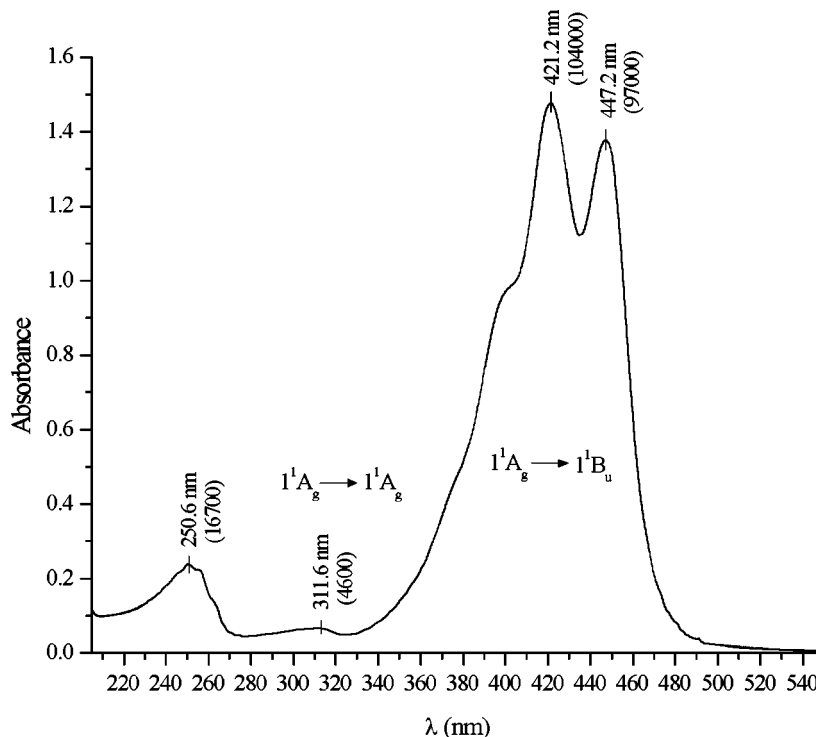


**Figure 2.** UV–vis absorption spectrum of crocetin at room temperature in borate buffer, pH 8.5. Concentration is  $1.5 \times 10^{-5} \text{ M}$ , optical pathlength is 1 cm.

bind to hydrophobic protein sites exhibiting highly polarizable microenvironment.<sup>18–21</sup> Therefore, this spectral shift can be utilized as a sign of carotenoid–protein binding. Our results clearly demonstrate that addition of albumin results in significant bathochromic shifts in the crocetin visible absorption spectrum (Fig. 3a–g) indicating the formation of carotenoid–protein complexes. As the protein concentration increases the vibronic band positions are shifted to longer wavelengths by 10–12 nm and plotting the wavelengths of the visible absorption maxima (nm) as a function of the albumin/crocetin molar ratio (Fig. 4) shows that above a 2:1 ratio only minor changes occur, suggesting that nearly all crocetin molecules are bound to albumin. The largest red shift was observed in the presence of pig albumin (421.2→433.6). In parallel with the spectral shifts, the absorption band shapes are also altered. The vibrational fine structure prominent in the free molecules is considerably decreased and the longest wavelength absorption peak becomes a shoulder upon albumin addition (Fig. 3a–g). These changes indicate the coexistence of free and protein-bound crocetin molecules having their absorption maxima at different positions. Coalescence of their spectra leads to the curves measured experimentally.

As the fraction of unbound molecules decreases and the bound species begin to dominate the vibrational fine structure appears again. Absorption spectra measured at the highest albumin concentrations represent carotenoid molecules embedded in the protein matrix and may be informative about the nature of the binding environment.<sup>22</sup> From this point of view, it is reasonable to compare the vibrational structures of the main absorption bands in the absence of albumin and at the largest albumin/crocetin ratio (10:1). To this end, the  $Abs_{\text{valley}}/Abs_{\text{max}}$  quotient was introduced, where  $Abs_{\text{valley}}$  is the value of absorption at the minimum between the two resolved peaks and  $Abs_{\text{max}}$  denotes the absorption at  $\lambda_{\text{max}}$ . For crocetin in a buffer solution this quotient is 0.76 and Table 1 shows the other values calculated from spectra of albumin–crocetin solutions (10:1). It is evident from these data and the visual inspection of the corresponding spectra (Fig. 3a–g) that the vibrational structure of human, rabbit, bovine and rat albumin–crocetin complexes are better resolved, suggesting the existence of some high affinity crocetin binding sites featured with well-defined rigid environment in which the conformational mobility of the crocetin molecules are considerably and similarly restricted.<sup>19</sup> On the other hand, the  $Abs_{\text{valley}}/Abs_{\text{max}}$  values are larger than 0.76 for horse, pig and dog albumin and their absorption bandwidths (FWHM value) measured at the half maxima are also significantly greater (Table 1). These results were interpreted by assuming that on horse, pig and dog albumin crocetin binds to heterogeneous, lower affinity sites with distinct geometry.<sup>22</sup>

While the absorption spectral changes reveal the sensitivity of crocetin to the surrounding media, the CD spectra reflects this sensitivity to an even greater extent. Lacking chiral groups, crocetin molecules show no optical activity when they are free in solution. However, when they are incorporated into an asymmetric environment such as the binding sites of the albumin molecule, induced optical activity may be observed. Above 300 nm albumin has no CD activity, therefore any CD band appearing in this region must be attributed to crocetin molecules bound in the chiral protein environment. Different types of CD activity were found with the seven albumin samples applied in the experiments. According to the  $S_0 \rightarrow S_2$  transition, typical vibronically coupled exciton band-pairs evolved for human and pig serum albumin that show opposite chirality (Fig. 3a,b). For HSA, the shape and magnitude of the left-handed exciton couplet is very similar to the one obtained with fatty acid-free human albumin<sup>7</sup> proving that the endogenous fatty acid molecules do not interfere substantially with the sites of crocetin binding (fatty acid-free dog and rabbit albumins also gave similar results to the respective non-fatty acid-free albumins; data not shown). As suggested in our previous work, excitonic interaction between two crocetin molecules bound to subdomain IIIA is the source of the observed spectrum.<sup>7</sup> As the albumin/crocetin ratio exceeds the value of 1, the magnitudes of both negative and positive bands begin to decrease due to the increasing fraction of albumin molecules binding only one crocetin molecule. As the albumin/crocetin ratio reaches a value of 10, the positive band completely disappears and only a negative ‘monosignate’ band can be seen (Fig. 3a). However, this band still comes from the excitonic interaction mentioned above and not from an asymmetrically perturbed single polyene chromophore because in the latter case the minima of the CD band would have been matching with the peak positions of the corresponding visible absorption band. Contrary to this, Table 2 and Fig. 3 show that is it not the case; rather the CD minima are in coincidence with the ones obtained at lower albumin concentrations. Additionally, since the intensity of the positive band is always smaller relative to its negative pair it becomes undetectable when the negative part still can be observed, again suggesting the presence of high affinity sites on HSA, binding in a cooperative manner.<sup>7</sup> Hence, a true isobestic point is not observed.

Like HSA, binding of crocetin to bovine albumin also results in a negative–positive, bisignate spectrum in the visible region (Fig. 3c). However, there are notable discrepancies between the two spectra including their shape and band intensities, respectively. For BSA at protein/ligand ratio of 1:3 only a positive band can be seen centered around 433 nm; with increasing albumin

**Figure 3.** Circular dichroism and absorption spectra of crocetin titrated with different kinds of serum albumin between 290–550 nm: (a) human, (b) pig, (c) bovine, (d) rat, (e) rabbit, (f) horse, (g) dog serum albumin. The concentration of crocetin varied from  $1.48 \times 10^{-5}$  M to  $1.15 \times 10^{-5}$  M upon added aliquots of albumin stock solutions For comparison, the absorption spectrum of crocetin measured in the absence of albumin is also presented.

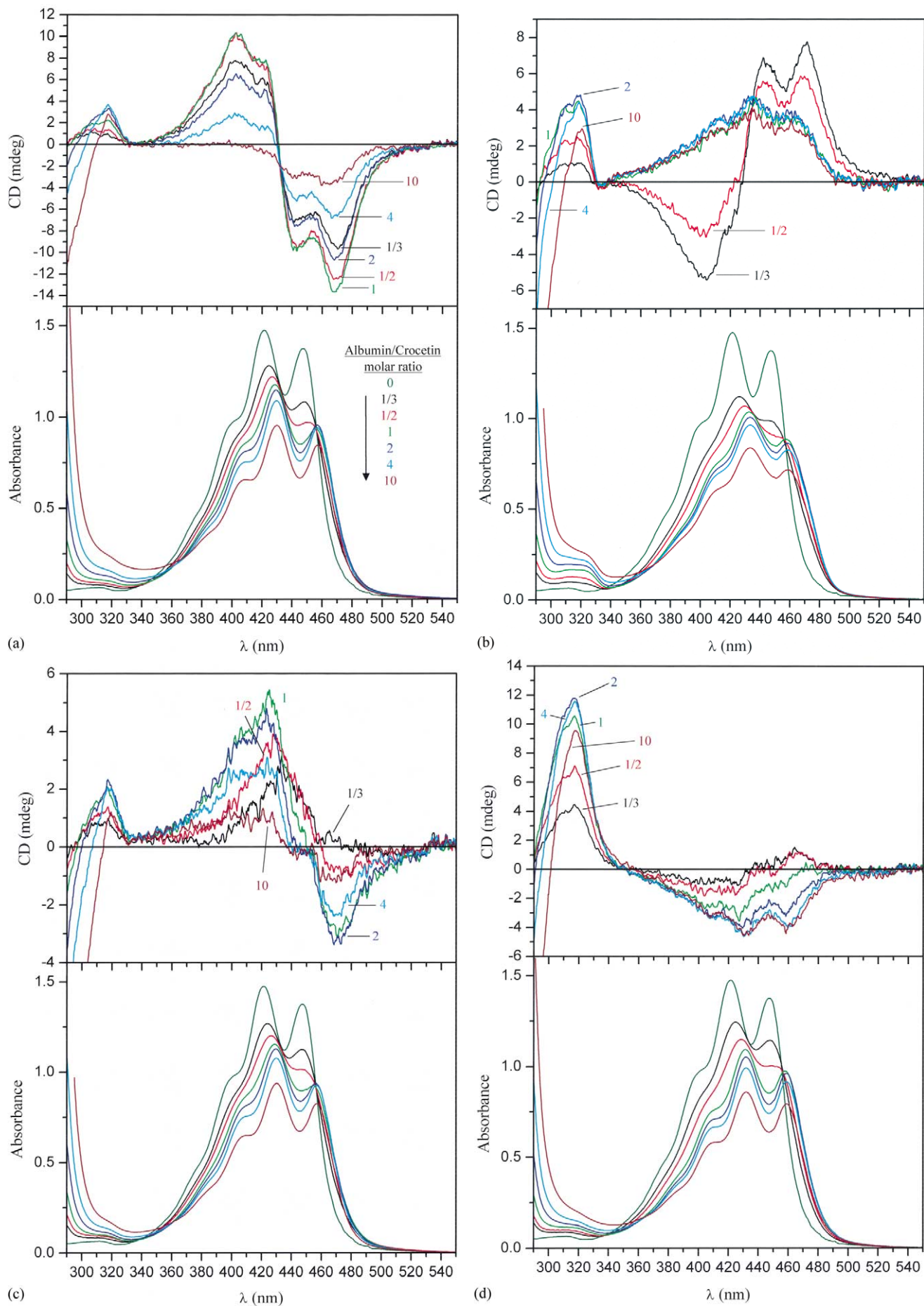


Fig. 3. (Continued)

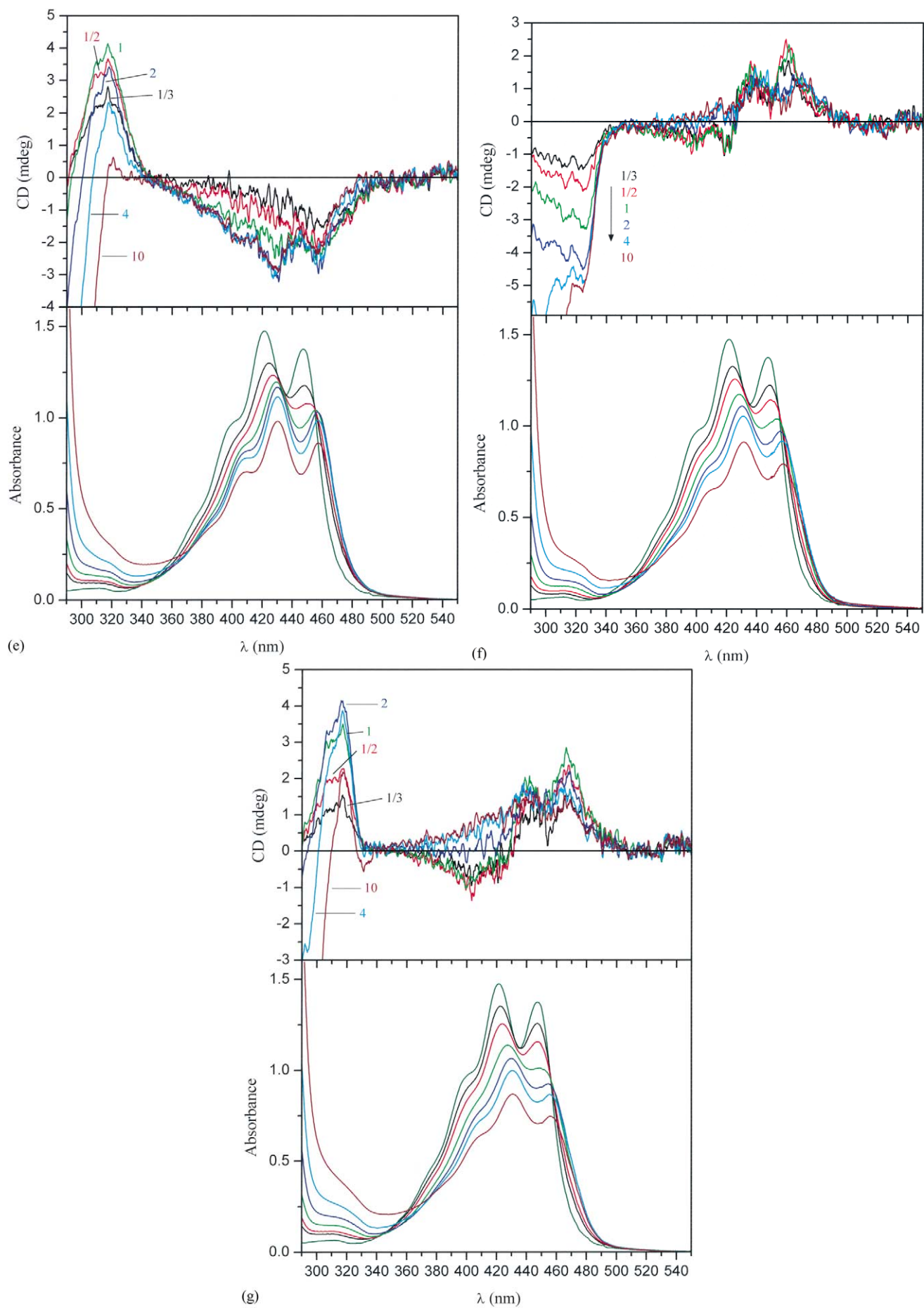
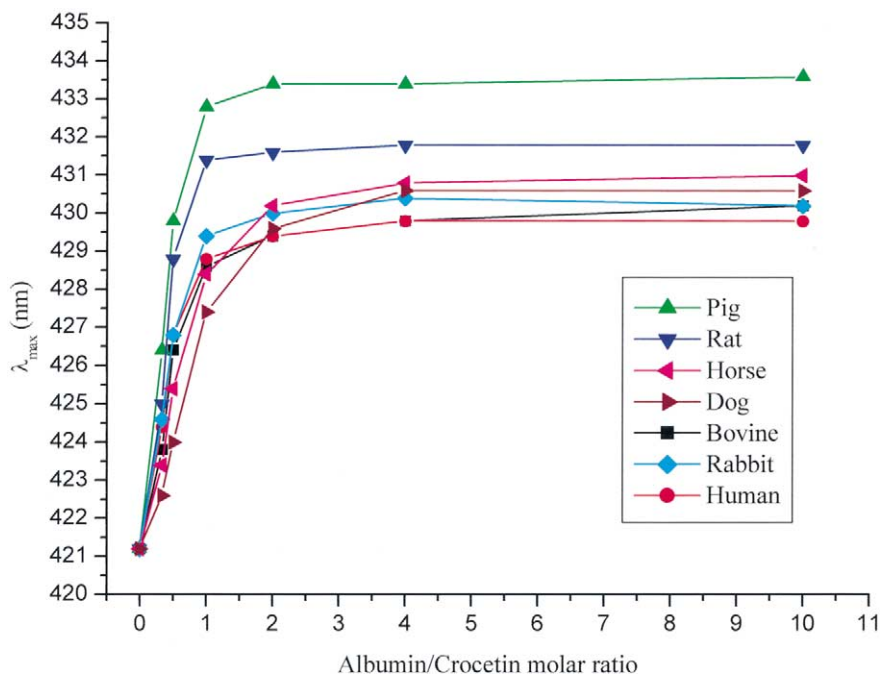


Fig. 3. (Continued)





**Figure 4.** The changes of the main visible absorption peak position (421.2 nm) of crocetin upon binding to serum albumin of different species.

**Table 1.** Comparison of the vibrational fine structure and bandwidth of the visible absorption bands of different crocetin–albumin complexes

	Dog	Pig	Horse	Crocetin in buffer solution at pH 8.5	Rat	Bovine	Rabbit	Human
$Abs_{\text{valley}}/Abs_{\text{max}}$	0.81	0.80	0.77	0.76	0.74	0.72	0.70	0.70
Full width at half maximum ( $\text{cm}^{-1}$ )	4283	4134	4058	3862	3964	3929	3984	3923

concentration a negative Cotton effect appears at about 470 nm and the positive band shifts to shorter wavelengths (Table 2). The zero crossover point is at about 450 nm while for HSA the same value is 430 nm; the wavelengths of the CD extrema do not match in the two cases and they are considerably weaker for BSA (Table 2). Additionally, the positive band is always more intense than the negative one. This spectral behavior is the consequence of the presence and mixing of two types of induced chirality: the positive Cotton effect found at 433 nm arises from a bound crocetin molecule being its  $1^1A_g \rightarrow 1^1B_u$  transition asymmetrically perturbed by the chiral environment of the protein;<sup>23</sup> on the other hand, similarly to HSA, a chiral exciton coupling occurs between two bound crocetin molecules positioning their long axes along a negative (left-handed) intermolecular angle. The coexistence of their CD signals results in a ‘mixed’ spectrum found experimentally. This can be proved by a simple arithmetical manipulation of the induced CD spectra of HSA– and BSA–crocetin complexes measured at 1:3 protein/ligand ratio. Adding the two curves after a normalizing procedure, the ‘anomalous’ bisignate spectrum of BSA–crocetin complex can be reconstructed (data not shown).

The pig albumin–crocetin complex behaves differently displaying opposite, right-handed exciton couplet being

in a mirror image relation with that of HSA (Fig. 3b, Table 2).

Furthermore, albumin addition has a striking effect on the CD spectrum. Instead of the gradual decrease, above a protein/ligand ratio of 0.5 the excitonic bands vanish and a new, positive, monosignate band arises with vibrational fine structure (Fig. 3b). Wavelength positions of its maxima and shoulders agree well with the corresponding values of the main absorption band and its intensity does not change significantly upon further albumin addition (Table 2). Moreover, the FWHM value and the  $Abs_{\text{valley}}/Abs_{\text{max}}$  quotient are significantly larger relative to that of HSA–crocetin complex (Table 1). All these spectral characteristics indicate that:

- on pig albumin the crocetin binding sites responsible for the exciton coupling have lower affinity;
- there are other, higher affinity site(s) binding a single carotenoid molecule in a chiral conformation resulting in helical distortion of the conjugated  $\pi$ -system.<sup>21,22,24</sup>

The helical twisting is a consequence of the ligand conformational adaptation to its binding environment and may occur through partial rotation around the formal  $-C=C-$  double or the  $=C-C=$  single bonds. How-

**Table 2.** Maxima and minima of the induced CD bands expressed in  $\Delta\epsilon$  ( $M^{-1} \text{ cm}^{-1}$ ) measured at different albumin–crocetin molar ratios (wavelength positions are italicized). For the calculations, dilution of the ligand concentration was considered

Albumin:crocetin molar ratio	Human	Pig	Bovine	Dog	Horse	Rabbit	Rat
<b>1:3</b>	−19.7 ( <i>470.4</i> )	+15.8 ( <i>471.2</i> )	+6.4 ( <i>433.2</i> )	+3.5 ( <i>468.6</i> )	+3.6 ( <i>460.2</i> )	−3.2 ( <i>460.6</i> )	+3.1 ( <i>464</i> )
	−14.7 ( <i>441.4</i> )	+14.1 ( <i>441.6</i> )		+2.6 ( <i>442.6</i> )	+2.4 ( <i>434.6</i> )		−2.3 ( <i>426.2</i> )
	+15.9 ( <i>402</i> )	−11.1 ( <i>404</i> )		−2.0 ( <i>403</i> )	−1.9 ( <i>418</i> )		
	+2.4 ( <i>306</i> )						
	+2.1 ( <i>317</i> )	+2.2 ( <i>318.4</i> )	+1.9 ( <i>317.2</i> )	+3.1 ( <i>317</i> )	−2.9 ( <i>321.8</i> )	+5.7 ( <i>317</i> )	+9.1 ( <i>317</i> )
<b>1:2</b>	−25.6 ( <i>467.6</i> )	+12 ( <i>469.4</i> )	−1.6 ( <i>472</i> )	+4.9 ( <i>467.6</i> )	+4.9 ( <i>458.8</i> )	−4.4 ( <i>455.6</i> )	+2.3 ( <i>466.2</i> )
	−19.7 ( <i>443.2</i> )	+11.5 ( <i>441.6</i> )	+7.8 ( <i>428.8</i> )	+3.5 ( <i>442</i> )	+3.5 ( <i>435.8</i> )		−3.4 ( <i>424.8</i> )
	+21.3 ( <i>402</i> )	−6.3 ( <i>403.4</i> )		−2.8 ( <i>403.2</i> )	−1.8 ( <i>418.2</i> )		
	+3.1 ( <i>308.2</i> )	+4.8 ( <i>309.2</i> )			−1.8 ( <i>396.4</i> )		
	+2.9 ( <i>317.8</i> )	+5.2 ( <i>317.2</i> )	+2.9 ( <i>317.2</i> )	+4.7 ( <i>317.4</i> )	−4.2 ( <i>324.8</i> )	+7.5 ( <i>317.2</i> )	+14.6 ( <i>317</i> )
<b>1:1</b>	−28.5 ( <i>467.2</i> )		−6.4 ( <i>470.4</i> )	+5.9 ( <i>466.2</i> )	+4.6 ( <i>460.8</i> )	−5.3 ( <i>455.4</i> )	
	−20.5 ( <i>443.2</i> )	+9.8 ( <i>437.2</i> )	+11.3 ( <i>425</i> )	+4.3 ( <i>441.8</i> )	+3.2 ( <i>436.4</i> )		−7.4 ( <i>424.2</i> )
	+21.5 ( <i>402</i> )			−2.1 ( <i>399.2</i> )	−1.6 ( <i>418.2</i> )		
	+4.1 ( <i>306.8</i> )	+8.7 ( <i>309.2</i> )					
<b>2:1</b>	+4.7 ( <i>317.2</i> )	+9.4 ( <i>318</i> )	+4.3 ( <i>316.8</i> )	+7.3 ( <i>317.2</i> )	−6.8 ( <i>326</i> )	+8.6 ( <i>317</i> )	+22 ( <i>317</i> )
	−22.9 ( <i>467.8</i> )		−7.3 ( <i>468.4</i> )	+4.7 ( <i>468.6</i> )	+3.0 ( <i>469.4</i> )	−6.4 ( <i>457.2</i> )	−6.9 ( <i>458.2</i> )
	−16.1 ( <i>443.6</i> )	+9.8 ( <i>435.8</i> )	+10.3 ( <i>423.2</i> )	+3.5 ( <i>442.8</i> )	+2.9 ( <i>435.8</i> )	−6.9 ( <i>430.8</i> )	−8.7 ( <i>429.4</i> )
	+14.1 ( <i>402.4</i> )						
<b>4:1</b>	+7.2 ( <i>318</i> )	+10.3 ( <i>319.2</i> )	+5.0 ( <i>317.2</i> )	+8.9 ( <i>316</i> )	−9.5 ( <i>324.6</i> )	+7.3 ( <i>318</i> )	+25.3 ( <i>317</i> )
	−15.4 ( <i>466.4</i> )		−5.3 ( <i>468.8</i> )	+3.8 ( <i>464</i> )	+2.8 ( <i>467</i> )	−6.1 ( <i>455.2</i> )	−9.2 ( <i>459.6</i> )
	−11.9 ( <i>443</i> )	+10.8 ( <i>434.6</i> )	+6.6 ( <i>423.8</i> )	+3.8 ( <i>437.6</i> )	+3.4 ( <i>438.6</i> )	−7.1 ( <i>427.2</i> )	−10.5 ( <i>430.2</i> )
	+6.6 ( <i>401.6</i> )						
<b>10:1</b>	+8.4 ( <i>317.2</i> )	+10.0 ( <i>318.2</i> )	+4.5 ( <i>317.8</i> )	+8.8 ( <i>316.8</i> )	−11.0 ( <i>324.8</i> )	+5.3 ( <i>317.4</i> )	+26.3 ( <i>317</i> )
	−9.6 ( <i>465.2</i> )		−3.2 ( <i>469.6</i> )	+3.5 ( <i>466.2</i> )	+3.0 ( <i>466.8</i> )	−6.2 ( <i>455.8</i> )	−11.7 ( <i>458.4</i> )
	−7.9 ( <i>442.8</i> )	+10.6 ( <i>435.8</i> )	+3.5 ( <i>421</i> )		+2.9 ( <i>438.6</i> )	−7.7 ( <i>430.4</i> )	−12.0 ( <i>430.4</i> )
	+7.4 ( <i>317.2</i> )	+7.8 ( <i>320.4</i> )	+3.2 ( <i>319.4</i> )	+5.7 ( <i>317.2</i> )	−13.2 ( <i>324.2</i> )	+1.7 ( <i>320.8</i> )	+25.1 ( <i>317.2</i> )

ever, there is an important difference between the two twist mechanisms regarding their effects on the  $1^1A_g \rightarrow 1^1B_u$  excitation energy. The  $=C-C=$  strain decreasing the conjugation, shifts the absorption maximum to shorter wavelengths while the  $-C=C-$  distortion, increasing the ground state and lowering the excited state energies, moves the absorption toward longer wavelengths.<sup>16,25</sup> Since the pig albumin–crocetin complex showed the largest bathochromic shift (Fig. 4) and one of the most intense monosignate Cotton band in the visible region (Table 2) it may be assumed that the  $-C=C-$  strain influences its CD and absorption spectra.

It is important to note that as with pig albumin, dog, horse and rat albumin–crocetin complexes also show a right-handed but very weak exciton couplet at lower protein/ligand ratios (Table 2). Parallel with the increasing albumin concentration, however, the amplitudes of the negative bands decrease and they completely disappear beyond the 1:1 albumin/crocetin ratio. In order to explain the distinct behavior of albumins regarding excitonic interaction, we first compared the amino acid compositions of the possible crocetin binding sites obtained from the X-ray crystallographic structure of HSA complexed with palmitic acid. Table 3 constructed by data from Refs. 10 and 12 shows the amino acid residues of HSA involved in the sites binding long-chain fatty acids together with analogous residues of the other albumins used in our experiments.

As concluded earlier,<sup>7</sup> binding of two crocetin molecules to the fatty acid sites 3 and 4 of subdomain IIIA might be the source of the observed intermolecular exciton coupling. The side chains responsible for hydrogen bonding with the carboxyl groups are very conserved between the two albumins except for the Ser-342 at site 3, which is replaced by Ala in BSA suggesting a possible answer as to why the induced CD is weaker in that case. Contrary to this, only very weak CD couplets were obtained for rat, horse and dog albumins although their Ser-342 is unchanged. For these albumins the cavity walls of site 3 and 4 are modified but it is difficult to imagine how such subtle changes can lead to a loss in excitonic activity. It must be emphasized, however, that the measure of excitonic interactions sensitively depend on the relative orientation of the interacting chromophores.<sup>8</sup> From this point of view, it is useful to investigate the molecular model obtained by fitting crocetin molecules to the long-chain fatty acid binding sites of HSA. According to Ref. 7, Fig. 5a shows two crocetin molecules bound within the fatty acid binding sites 3 and 4 of subdomain IIIA thought to be responsible for the left-handed (negative) exciton chirality (for clarity, the protein environment is omitted). Determined by the stereochemistry of the albumin binding sites 3 and 4, these molecules are arranged in such a position that makes their chiral interaction sensitive to modest changes in the intermolecular geometry.

**Table 3.** Amino acids of the binding cavity of long-chain fatty acids in HSA determined by X-ray crystallographic investigations compared with analogous residues of the five albumins used in the work (amino acids are denoted with their one-letter codes). Only the different residues have been shown

	Site 1 <i>Binding location: IB</i>		Site 2 <i>Binding location: IA-IB-IIA</i>		Site 3 <i>Binding location: IIIA</i>		Site 4 <i>Binding location: IIIA</i>		Site 5 <i>Binding location: IIIB</i>	
	Side chains for H-bonding	Residues lining cavity wall	Side chains for H-bonding	Residues lining cavity wall	Side chains for H-bonding	Residues lining cavity wall	Side chains for H-bonding	Residues lining cavity wall	Side chains for H-bonding	Residues lining cavity wall
Human	<b>IB:</b> R117	<b>IB:</b> R117, P118, M123, F134, Y138, L139, I142, F157, A158, Y161, F165, L182	<b>IB:</b> Y150 <b>IIA:</b> R257, S287	<b>IA:</b> V7, R10, L14, F19, L22, L66 <b>IB:</b> A151, P152 <b>IIA:</b> L250, L251, A254, A258, L283, L284	<b>IB:</b> S342, R348 <b>IIIA:</b> R485	<b>IB:</b> V344, L345 <b>IIIA:</b> P384, L387, I388, F403, L430, V433, K439, M446, A449, E450, L453, R485	<b>IIIA:</b> R410, Y411, S419, T422, S489	<b>IIIA:</b> Y411, V415, V418, T422, L423, V426, L430, L453, L457, L460, V473, R485, F488, L491	<b>IIIA:</b> Y401 <b>IIIB:</b> K525	<b>IIIB:</b> F502, F507, F509, K525, A528, L529, L532, V547, M548, F551, L575, V576, S579, L583
Bovine	K117	K117, L123, Y157, I182		<b>IA:</b> I7	<b>IB:</b> A342	<b>IB:</b> S344, V345 <b>IIIA:</b> T439, T449				T579
Pig	K117	K117, L123, Y157, I182		<b>IA:</b> I7, I66		<b>IB:</b> S344 <b>IIIA:</b> L446, A449				L548, F575, I579
Rat		V142, Y157, L165		<b>IA:</b> I7, I66 <b>IIA:</b> V283		<b>IB:</b> S344 <b>IIIA:</b> V388, T439, L446, V449	A415, A426			
Horse	K117	K117, Q123, V142, H157		<b>IA:</b> I7 <b>IB:</b> G151		<b>IB:</b> S344 <b>IIIA:</b> V388, L446, S449	A415, I426, I473			L548
Dog	A117	A117, L123, Y157, I182		<b>IA:</b> I7 <b>IB:</b> S151 <b>IIA:</b> V283		<b>IB:</b> S344 <b>IIIA:</b> V388	A415			A579

Moving the site 4 ligand towards the center of the site 3 molecule, a nearly achiral molecular arrangement can be obtained in which the left- and right-handed excitonic interactions cancel each other out (Fig. 5b). Upon further replacement of the site 4 molecule the chirality appears again but with opposite sense since there is a positive (clockwise) intermolecular twist between the long axes of the crocetin molecules (Fig. 5c) resulting in a mirror image CD spectrum. According to this model, there is no need for profound changes in the ligand binding sites for such molecular reorientations but distant sequence alterations might modify the tertiary structure leading to a markedly different intermolecular

arrangement. According to our molecular modeling studies on HSA–crocetin complex,<sup>7</sup> no other combination of two crocetin binding sites was found within which a similar small change in the intermolecular geometry would lead to inversion of the exciton chirality.

Between 316 and 325 nm, all CD spectra display an induced, positive or negative Cotton band with various intensity, closely matching with the *cis*-peak in the near ultraviolet region (Fig. 3a–g, Table 2). The observed CD bands prove that the *cis*-isomers of crocetin are also able to bind with the serum albumins and they



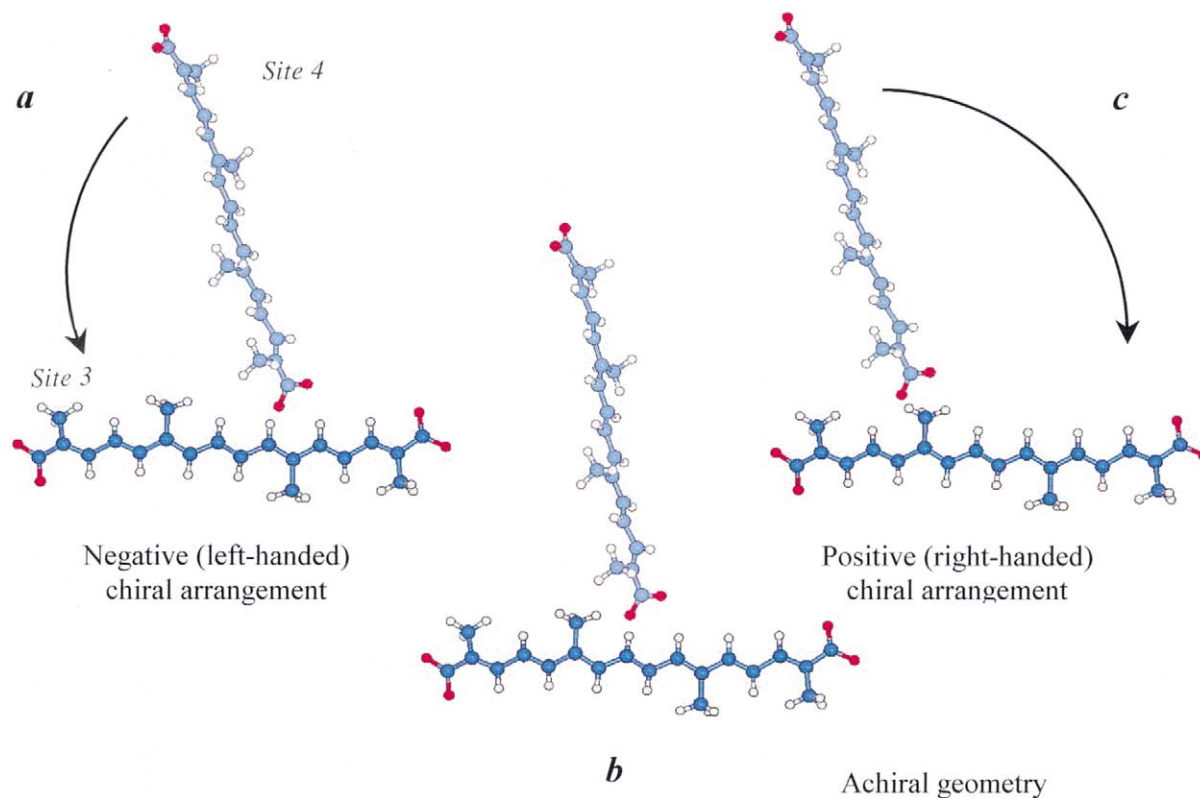


**Figure 5.** (a) Molecular model of the left-handed intermolecular positions of crocetin molecules fitted to the long-chain fatty acid binding sites 3 and 4 in subdomain IIIA.<sup>7</sup> (b) and (c) Illustration of spatial shifting of the site 4 molecule from which results first a nearly achiral intermolecular arrangement accounted for a no or very weak exciton coupling (dog, rat, horse and rabbit albumins), then a positive (right-handed) intermolecular angle resulting oppositely signed exciton bands as measured with the pig albumin–crocetin complex.

become optically active since the asymmetric protein environment enforces a twisting around the *cis*-bond producing a non-planar helical conformer. The *cis*-bond is located peripherally (i.e. 9'-*cis* or 11'-*cis*, see Fig. 2) because in the case of central mono *cis* configuration the transition dipole moments belonging to the  $\pi$ -systems of the two parts separated by the *cis*-bond would excitonically interact with each other resulting in a bisignate CD band in the near ultraviolet region.<sup>24</sup> To determine the molecular helicity, the so-called  $C_2$ -chirality rule can be applied that has been elaborated for a twisted diene model and generalized later to several chromophores of  $C_2$ -symmetry.<sup>26,27</sup> Although the peripheral mono-*cis*-isomers of crocetin only have pseudo- $C_2$ -symmetry, theoretical calculations and experimental data proved the rule to be valid in such a case too.<sup>27</sup>

According to the rule, in the case of left-handed chiral conformation the Cotton effect belonging to the *A* transition symmetry ( $1^1A_g \rightarrow 1^1A_g$ ) is positive, while for the *B* transition symmetry ( $1^1A_g \rightarrow 1^1B_u$ ) is negative and vice versa. In this context, the term 'left-handed' means a negative (counterclockwise) torsional angle around the *cis*-bond. CD spectra obtained in the presence of rat, rabbit and horse albumin obey this rule (Fig. 3d–f) suggesting *cis*-isomers bind in a left- or right-handed conformation, respectively.

### 3. Experimental

#### 3.1. Materials

Bovine, dog, horse, human, pig, rabbit and rat serum albumin (catalog numbers are A-2153, A-9263, A-9888, A-9511, A-2764, A-0639, A-6772, respectively) were purchased from Sigma Co., and used as supplied. All protein samples were non-fatty acid free and obtained from the serum fraction V. For comparison, CD titration experiments were also performed with fatty acid free human, dog and rabbit serum albumin samples, but no spectroscopic differences were found relative to the corresponding non-fatty acid free samples. According to the certificate of analysis provided by Sigma, purity data of albumin samples are listed below.

Human serum albumin (Lot No. 127F9320): approx. 99% purity (agarose electrophoresis); water content 1.8%.

Human serum albumin, fatty acid free (catalog No. A-1887, Lot No. 14H9319): approx. 97% purity (agarose electrophoresis); free fatty acids 0.005%; water content 2.6%.

Bovine serum albumin (Lot No. 67H0357): >98% purity (agarose electrophoresis).

Pig serum albumin (Lot No. 64H9309): 98% purity (agarose electrophoresis); water content 6.6%.

Dog serum albumin (Lot No. 21H9304): 100% purity (immunoagarose electrophoresis); water content 3.7%.

Dog serum albumin, fatty acid free (catalog No. A-3184, Lot No. 21H9316): >99% purity (agarose electrophoresis); free fatty acids 0.002%.

Rabbit serum albumin (Lot No. 13H9321): >99% purity (agarose electrophoresis); water content 4.6%.

Rabbit serum albumin, fatty acid free (catalog No. A-9438, Lot No. 13H9321): >99% purity (agarose electrophoresis); water content 3.1%; free fatty acids 0.004%.

Horse serum albumin (Lot No. 37F9326): 99.5% purity (immunoagarose electrophoresis); water content 1.5%.

Rat serum albumin (Lot No. 84H9331): 98.7% purity (immunoagarose electrophoresis); water content 2.7%.

A value of 66 kDa was used as a mean molecular weight to prepare albumin stock solutions (i.e. 1 mg/ml  $\approx 1.5 \times 10^{-5}$  molar concentration).

UV absorption spectra of the albumin samples in the range of 250–350 nm were recorded; the absorbance values at 280 nm are collected in Table 4 together with the occurrence of tryptophan and tyrosine residues in the respective species. These are responsible for the measured absorption ( $\epsilon_{280 \text{ nm}} = 5540$  [tryptophan], and 1480 [tyrosine]). It can be seen that the order of absorbance values is in fairly good agreement with the order of availability of these aromatic amino acids in the respective species.

Crocin pyridine salt (C-3398, approx. 95% purity grade) was obtained from Sigma and used without further purification. To prepare the spectroscopic samples, albumin and crocin samples were dissolved in a 0.2 M borate/boric acid buffer at pH 8.5.

### 3.2. Absorbance and CD measurements

CD and UV-vis spectra were recorded on a Jasco J-715 spectropolarimeter at  $25 \pm 0.2^\circ\text{C}$  in a rectangular cuvette with a 1 cm pathlength. Temperature control was

provided by a Peltier thermostat equipped with magnetic stirring. All spectra were accumulated five times with a bandwidth of 1.0 nm and a resolution of 0.2 nm at a scan speed of 100 nm/min.

### 3.3. CD/UV-vis titration of crocin with HSA

A 1 cm cuvette was filled with 2 ml  $1.5 \times 10^{-5}$  M crocin solution. After recording the CD and absorbance spectra between 205 and 550 nm, 20, 10, 30, 60, 120 and 360  $\mu\text{l}$   $5 \times 10^{-4}$  M albumin stock solutions were added consecutively to achieve 1:3, 1:2, 1:1, 2:1, 4:1 and 10:1 albumin/crocin molar ratios, respectively. The final crocin concentration was  $1.15 \times 10^{-5}$  M.

### Acknowledgements

Helpful discussions with Dr. Ilona Fitos are gratefully acknowledged. This work was supported by the Hungarian National Scientific Fund (OTKA T 033109).

### References

- Winterhalter, P.; Straubinger, M. *Food Rev. Int.* **2000**, *16*, 39–59.
- Ríos, J. L.; Recio, M. C.; Giner, R. M.; Mánez, S. *Phytother. Res.* **1998**, *10*, 189–193.
- Jagadeeswaran, R.; Thirunavukkarasu, C.; Gunasekaran, P.; Ramamurthy, N.; Sakthisekaran, D. *Fitoterapia* **2000**, *71*, 395–399.
- Chang, W. C.; Lin, Y. L.; Lee, M. J.; Shioh, S. J.; Wang, C. J. *Anticancer Res.* **1996**, *16*, 3603–3608.
- Escribano, J.; Alonso, G. L.; Coca-Prados, M.; Fernandez, J. A. *Cancer Lett.* **1996**, *100*, 23–30.
- Singer, M.; Stidwill, R. P.; Nathan, A.; Gainer, J. L. *Crit. Care. Med.* **2000**, *28*, 1968–1972.
- Zsila, F.; Bikádi, Z.; Simonyi, M. *Tetrahedron: Asymmetry* **2001**, *12*, 3125–3137.
- Berova, N.; Nakanishi, K. In *Circular Dichroism: Principles and Applications*; Berova, N.; Nakanishi, K.; Woody, R. W., Eds. Exciton chirality method: principles and application; Wiley-VCH: New York, 2000; pp. 337–382.
- Miller, T. L.; Willett, S. L.; Moss, M. E.; Miller, J.; Belinka, B. A. *J. Pharm. Sci.* **1982**, *71*, 173–177.
- Bhattacharya, A. A.; Grune, T.; Curry, S. *J. Mol. Biol.* **2000**, *303*, 721–732.

**Table 4.** Comparison of the occurrence of tryptophan and tyrosine residues in the albumin species studied and their absorbance at 280 nm (Concentration of all samples is 1 mg/ml  $\approx 1.5 \times 10^{-5}$  M, optical pathlength is 1 cm, pH 8.5)

Albumin source	No. of tryptophan residues	No. of tyrosine residues	Absorbance at 280 nm
Pig	2	22	0.604
Bovine	2	20	0.591
Rabbit	1	22	0.568
Rat	1	21	0.530
Dog	1	21	0.507
Human	1	18	0.520
Horse	1	17	0.474

11. Curry, S.; Brick, P.; Franks, N. P. *Biochim. Biophys. Acta* **1999**, *1441*, 131–140.
12. Curry, S.; Mandelkow, H.; Brick, P.; Franks, N. *Nat. Struct. Biol.* **1998**, *5*, 827–835.
13. Peters, T. *All About Albumin: Biochemistry, Genetics and Medical Applications*; Academic Press: San Diego, 1996; pp. 55–83.
14. Ho, J. X.; Holowachuk, E. W.; Norton, E. J.; Twigg, P. D.; Carter, D. C. *Eur. J. Biochem.* **1993**, *215*, 205–212.
15. Kohler, B. E. In *Carotenoids Volume 1B: Spectroscopy*; Britton, G.; Liaaen-Jensen, S.; Pfander, H., Eds. Electronic structure of carotenoids; Birkhäuser: Basel, 1995; pp. 1–13.
16. Hu, Y.; Hashimoto, H.; Moine, G.; Hengartner, U.; Koyama, Y. *J. Chem. Soc., Perkin Trans. 1* **1997**, 2699–2710.
17. Kuki, M.; Nagae, H.; Cogdell, R. J.; Shimada, K.; Koyama, Y. *Photochem. Photobiol.* **1994**, *59*, 116–124.
18. Yan, B.; Spudich, J. L.; Mazur, P.; Vunnam, S.; Derguini, F.; Nakanishi, K. *J. Biol. Chem.* **1995**, *270*, 29668–29670.
19. Jouni, Z. E.; Wells, M. A. *J. Biol. Chem.* **1996**, *271*, 14722–14726.
20. Davis, C. M.; Bustamante, P. L.; Loach, P. A. *J. Biol. Chem.* **1995**, *270*, 5793–5804.
21. Ruban, A. V.; Pascal, A. A.; Robert, B. *FEBS Lett.* **2000**, *477*, 181–185.
22. Ruban, A. V.; Pascal, A. A.; Robert, B.; Horton, P. *J. Biol. Chem.* **2001**, *276*, 24862–24870.
23. Zhang, H.; Huang, D.; Cramer, W. A. *J. Biol. Chem.* **1999**, *274*, 1581–1587.
24. Koyama, Y.; Hashimoto, H. In *Carotenoids in Photosynthesis*; Young, A.; Britton, G., Eds. Spectroscopic studies of carotenoids in photosynthetic systems; Chapman & Hall: London, 1993; pp. 327–408.
25. Buchwald, M.; Jencks, W. P. *Biochemistry* **1968**, *7*, 844–859.
26. Hug, W.; Wagnière, G. *Tetrahedron* **1972**, *28*, 1241–1248.
27. Sturzenegger, V.; Buchecker, R.; Wagnière, G. *Helv. Chim. Acta* **1980**, *63*, 1074–1092.